

ADAPTIVE PARAMETER TUNING FOR MORPHOLOGICAL SEGMENTATION OF BUILDING FACADE IMAGES

Andrés Serna, Jorge Hernández and Beatriz Marcotegui

Mines ParisTech
 CMM - Centre de morphologie mathématique
 Mathématiques et Systèmes
 35 rue St Honoré 77305-Fontainebleau-Cedex, France

ABSTRACT

We present an adaptive method to segment Haussmanian facades from street level images. Our approach assumes that images are rectified, cropped and their elements are aligned in a pseudo-regular structure. It is based on the accumulation of directional color gradients, combined with morphological filters in order to deal with textured facades. We propose an automatic parametrization of three filters included in the process: opening filter of size n_{op} , alternate sequential filter (ASF) of size n , and H-minima filter with contrast threshold h . This automatic selection offers robustness to noise, image resolution changes, shadows and textures. Quantitative and qualitative results are reported on a public annotated database, validating the good performances of our approach.

Index Terms— Mathematical morphology, facade segmentation, window detection, urban modeling

1. INTRODUCTION

Digital 3D city models are useful for many applications: urban planning, emergency response simulation, cultural heritage documentation, virtual tourism, route planning, studies of accessibility for disabled people, among others. Thanks to availability of new types of 3D data, an increasing number of geographic applications such as Google Earth, Microsoft Virtual Earth and Geoportail are flourishing nowadays. Some of these applications do not only require to look realistic, but also have to be faithful to reality.

Initially, virtual scenarios were created by infographic approaches, leading to time-consuming procedures, unsuitable for large-scale urban modeling. Procedural modeling allows to speed up the 3D virtual environment creation [1]. It is based on a set of rules, a grammar, defin-

ing a given architectural style. Procedural modeling approaches create realistic models in an efficient way, but a precise parametrization is required if the model has to be faithful to reality. Automatic analysis of facade images, combined with procedural modeling, allows to increase the productivity while remaining faithful to reality.

Many algorithms focusing on automatic facade analysis have been designed in the recent years. In general, existing methods use rectified and cropped images containing a single building. Usually, individual buildings are manually extracted. In [2], Lee and Nevatia develop a method based on thresholding of directional gradient projections. In [1], Müller et al. find repetitive architectural structures using mutual information to describe a single facade image. These methods are very sensitive to noise and fail if the building contains textured walls or balconies with different wrought iron designs, very common elements in Parisian Haussmannian architecture. In [3], Hernández et al. describe a method that automatically extracts an isolated building from a city block street level image. Besides, they extend Lee and Nevatia method introducing morphological filters in the directional gradient projections. These filters improve the robustness to textured facades. In [4], Teboul et al. learn a shape dictionary using random forest technique and publish an annotated database with 100 building images. In [5], Hammoudi extracts facade structures from 3D point clouds data using Hough transform. Finally, in [6], Pinte et al. combine color information and 3D point cloud data to improve the method robustness.

In this paper we focus on morphological directional gradient projections combined with morphological filters. We study the adaptive parameter tuning of these filters and evaluate the proposed algorithm on the cited public database. The paper is organized as follows. Section 2 describes the morphological directional gradient projection technique, illustrated on a vertical splitting example. Section 3 describes the filter parametrization technique. Section 4 shows the performance of our method

{andres.serna_morales, jorge.hernandez, beatriz.marcotegui}
 @mines-paristech.fr

on Teboul’s annotated database. Finally, Section 5 is devoted to conclude this work.

2. SEGMENTATION OF BUILDING FACADES

The starting point for our approach is the method developed by Hernández et al. [3]. Input images are assumed rectified and cropped, as shown in Fig. 2(b). Fig. 1 shows the diagram of the whole process and Fig. 2 illustrates intermediate images. First, a morphological vertical gradient $G_y(x, y)$ detects horizontal contours (Fig. 2(c)). Then, a horizontal opening filter of size n_{op} is applied in order to eliminate the undesirable details. Fig. 2(e) shows the accumulation, column by column, of the vertical gradient. This 1D projected gradient contains peaks at window locations and valleys between them.

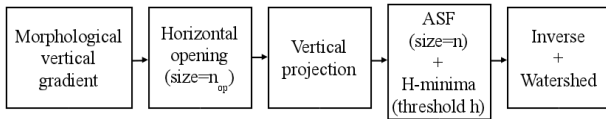


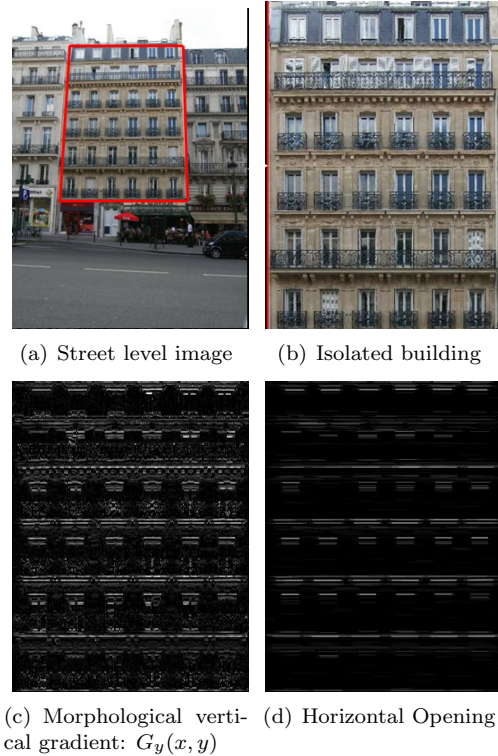
Fig. 1. Process scheme to compute vertical divisions.

Afterwards, this projection is filtered in order to get a single maximum for each window. An Alternate Sequential Filter (ASF) of size n and a H-minima filter are used for this purpose. Finally, this profile is inverted and a watershed process computes the facade division. Fig. 2(f) shows the final result superimposed on the original image. Although a vertical splitting is shown, the same technique applies to horizontal splitting, just changing vertical by horizontal and vice versa.

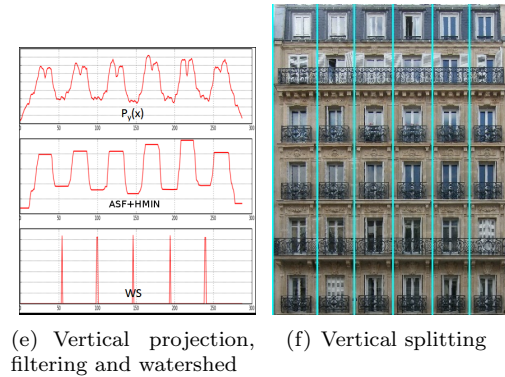
A frequency domain analysis of this profile would also be possible, but our approach is more robust to pseudo-periodic structures. Fig. 3 shows some qualitative results demonstrating the robustness of our method to occlusions, shadows and rectification problems. Note that our method is robust to rectification errors as long as a line can pass through the wall without touching any window.

3. FILTERING PARAMETRIZATION

The method introduced in the previous section leads to interesting results but relies on a good filter parametrization. Specifically, three parameters require tuning: the size n_{op} for the horizontal opening, the size n for the ASF, and the contrast threshold h for the H-minima filter. If these parameters are too small, the result will be over-segmented (Figures 5(a) and 5(b)). On the other hand, if they are too big, the result will be under-segmented (Fig. 5(d)). The aim of this section is to tune in an adaptive way these filter parameters, according to



(a) Street level image (b) Isolated building (c) Morphological vertical gradient: $G_y(x, y)$ (d) Horizontal Opening



(e) Vertical projection, filtering and watershed (f) Vertical splitting filtering and watershed

Fig. 2. Vertical splitting. Image from [3].

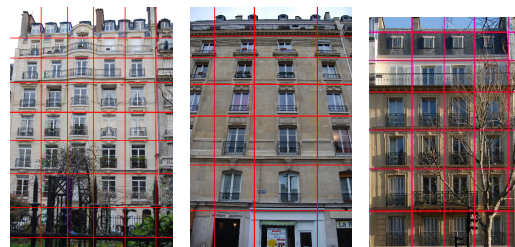


Fig. 3. Facade divisions. Images from [3].

intrinsic image information. The parameter tuning of each step is explained below.

3.1. Opening filter parametrization

Windows are the image largest structures. Small details such as facade ornaments, wrought iron balconies or other noisy structures can produce fake divisions on projected profile $P_y(G_y)$. A morphological opening with a horizontal structuring element of size n_{op} is used in order to get rid of these details from gradient images. The selection of n_{op} is based on the pattern spectrum [7, 8]. Pattern spectrum (PS) plots the quantity of information filtered out by each opening γ_i : ($PS_i = \sum_{\forall pixel} (\gamma_{i-1} - \gamma_i)$). The resulting curve is also called *size distribution* because its peaks correspond to the prevailing sizes of the image structures.

Fig. 4 shows size distributions for different $G_y(x, y)$ images. These curves present an important peak for small size openings. This peak corresponds to noisy details. Note that this peak exists for the three images in spite of shadows (Fig. 10(e)), balconies (Fig. 10(b)), and vegetation (Fig. 10(d)). The opening size is chosen as the value i for which the pattern spectrum falls down under 25% of its maximum. This selection offers robustness to image resolution changes.

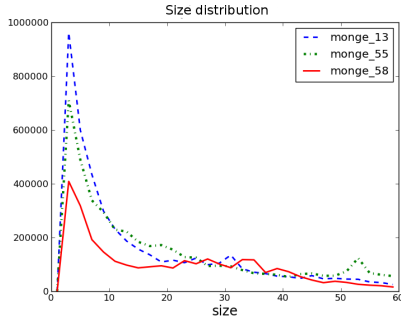


Fig. 4. Size distribution of $G_y(x, y)$ with a horizontal structuring element. Test images correspond to Fig. 10.

3.2. ASF filter parametrization

An ASF consists in a sequence of openings (γ) and closings (φ) of increasing sizes. The sequence starts with the filter of size 1 and ends with the filter of size n : $ASF_n(P_y(G_y)) = \gamma_n \varphi_n \dots \gamma_2 \varphi_2 \gamma_1 \varphi_1(P_y(G_y))$. This filter is particularly appropriated when the noise is present over a wide range of scales [9]. The filter size is chosen based on the facade regularity. Several filters of different sizes are applied, and the one leading to the most regular result is chosen. The regularity is estimated by the standard deviation σ of the segmented facade division sizes. This filter is applied to 1D profiles. Thus, evaluating different sizes is not a time-consuming task.

Fig. 5 shows the resulting vertical divisions for different filter sizes. Note that the filter size that minimizes the standard deviation, $n=7$, leads to a correct facade division.

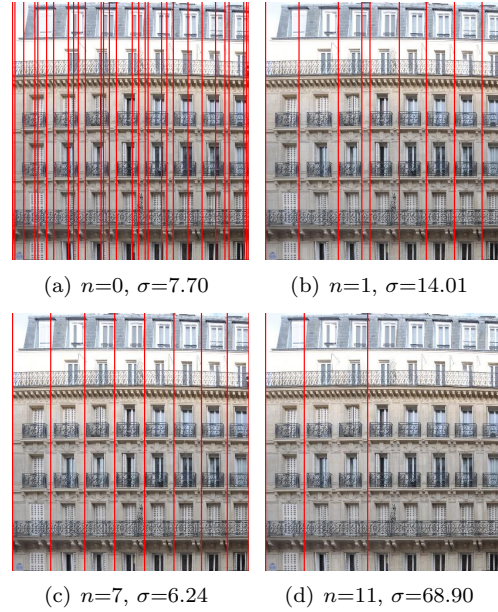


Fig. 5. Divisions for different ASF sizes. Image from [3].

3.3. H-minima filter parametrization

H-minima filter is a filtering tool based on a contrast criterion. More precisely, this transformation suppresses all minima whose contrast is lower than a given threshold h [10]. The contrast threshold h is chosen as a percentage of the dynamic of the extrema in the profile, that is $h \propto \max(f) - \min(f)$, where $f = ASF_n(P_y(G_y))$. This adaptive selection provides independence with respect to image resolution. Fig. 6 illustrates the effect of ASF and H-minima filtering. Note that the strongest filtering is carried out by the ASF, while the H-minima removes still remaining possible low contrasted extrema, as shown in the left side of Fig. 6.

3.4. Window detection

We assume that there is only one column of windows per vertical division. Analyzing the extrema of the filtered profile $\tilde{P}_y(G_y)$, we found that minima pass through the wall while maxima pass through the windows. Using this information, we apply a constrained watershed on the projected horizontal gradient $P_y(G_x)$, taking the extrema of $\tilde{P}_y(G_y)$ as markers. Fig. 7 illustrates the process of window detection.

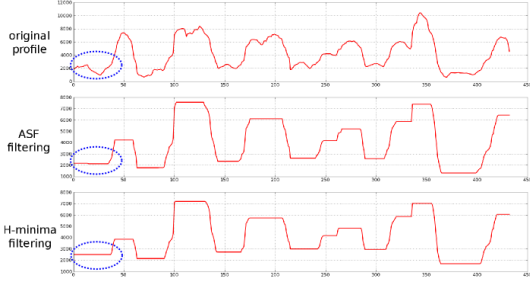


Fig. 6. ASF and H-minima filtering. The original profile corresponds to Fig. 10(a).

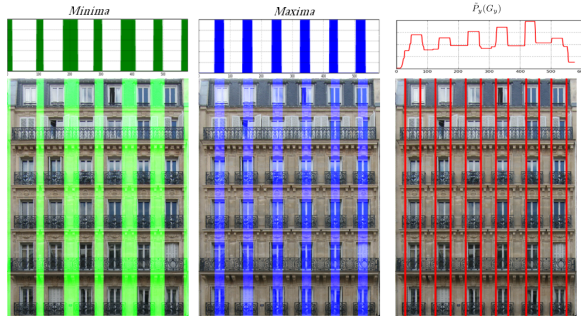


Fig. 7. Location of the vertical edge of the windows.

4. EXPERIMENTS

Our method is tested on the public database [4] that contains 100 images. Images are rectified and various semantic elements are manually annotated. An example is shown in Fig. 8. We evaluate our system on window localization with the classic precision (P), recall (R) and f_{mean} criteria. P is the fraction of retrieved instances that are relevant, R is the fraction of relevant instances that are retrieved taking all relevant instances in the database into account, and $f_{mean} = 2PR/(P + R)$.

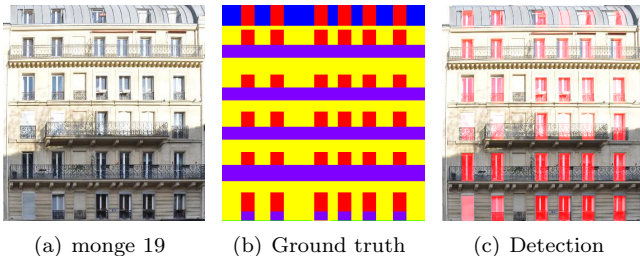


Fig. 8. Example of an annotated image from [4].

Note that our procedure detects windows including their corresponding balconies. In order to evaluate cor-

rectly the window detection performance, we remove from our detection the ground truth balconies regions. Fig. 9(a) shows the evaluation scores obtained with increasing ASF sizes. We can observe that the maximum $f_{mean}=0.79$ corresponds to filters of size between 7 and 10. If we use the ASF fitting method proposed in Section 3.2, we get the same score, the maximum in the figure, which proves the efficiency of the proposed tuning.

Once the parameters n_{op} and n are chosen according to the procedure aforementioned, we need to choose the best h threshold for the H-minima filter. Fig. 9(b) shows an exhaustive test varying h from 1% to 30% of the dynamic in the profiles. The best values found in the test correspond to $h_v=14\%$ and $h_h=2.5\%$ of the dynamic for the vertical and horizontal filter thresholds, respectively. Note that this parameter is not so critical since the lowest and highest f_{mean} correspond to 0.78 and 0.80, respectively. However, it improves the global performance up to 1% with respect to Fig. 9(a), where H-minima filter is not applied.

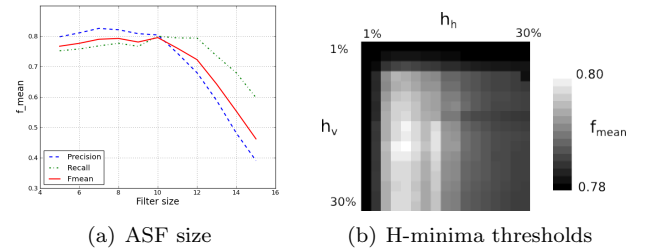


Fig. 9. f_{mean} sensitivity to parameters n , h_h and h_v .

The results reported by Teboul et al. are $P = 0.65$, $R = 0.81$ and $f_{mean} = 0.72$, these figures are computed from the confusion matrix of [4] considering windows and balconies in the same category. However, they only test 10 images of the database, while we have run our experiments on the whole dataset.

Using our proposed adaptive parameter tuning, the results are $P = 0.82$, $R = 0.79$ and $f_{mean} = 0.80$, which is much better than other results reported in the literature on the public Teboul's database. Qualitative results are shown in Fig. 10. Figures 10(a), 10(b) and 10(c) show examples in which the proposed method fails. Those images do not respect the regularity hypothesis on which our system is based: some window columns are almost adjacent. The standard deviation of division width is smaller when those columns are merged than when they are separated. Figures 10(d), 10(e) and 10(f) present the robustness of our system to shadows, textures and images on which the distance between windows are pseudo-regular.



Fig. 10. Examples of results. Images from [4].

Although developing a real time application is out of this work scope, the process takes approximatively 0.7 seconds per image on an Intel(R) Core(TM) i7 CPU 2.93 GHz and 8 GB memory desktop computer.

5. CONCLUSIONS

We propose an automatic parameter tuning of the three filters in the process: i) size n_{op} of the opening filter is deduced from the pattern spectrum analysis of gradient images. This filter removes texture details on the facade in order to avoid fake divisions. Moreover, its adaptive tuning offers robustness to image resolution changes. ii) Size n of the ASF is chosen as the value that minimizes the standard deviation σ of the segmented region sizes. This filter size has a strong influence on the result, as shown in Fig. 5. Its adaptive tuning leads to the best result among all filter sizes. And, iii) contrast threshold h in the H-minima filter is chosen as a percentage of the dynamic of the extrema in the profile. The sensitivity to this parameter is very low, that means that the spurious maxima remaining after the ASF are very low contrasted, as shown in Fig. 6. This filter improves f_{mean} criterion by 1% (from 79% to 80%).

The adaptive parameter tuning offers robustness to noise, image resolution changes, shadows and textures. These adaptive filters lead to the best performance score compared to any filter parameters tested in an exhaustive way. If the database resolution had been heterogeneous, the results would have been even better than the score with any filter parameter, because our parameters would

have been adapted to each image size. Qualitative and quantitative results are reported. Our performances are better than others reported in the literature on Teboul's public database. Thus, our approach is validated.

In the future, the use of an adaptive opening operator, called ultimate opening, will be studied. This operator automatically adapts its size to the image structures, based on a contrast criterion.

6. ACKNOWLEDGEMENTS

The work reported in this paper has been performed as part of Cap Digital Business Cluster TerraNumerica project.

7. REFERENCES

- [1] P. Müller, G. Zeng, P. Wonka, and L. Van Gool, "Image-based procedural modeling of facades," *ACM Transactions on Graphics*, vol. 26, no. 3, pp. 85–93, 2007.
- [2] S. C. Lee and R. Nevatia, "Extraction and integration of window in a 3d building model from ground view images," *IEEE Computer Vision and Pattern Recognition*, vol. 02, pp. 113–120, 2004.
- [3] J. Hernández and B. Marcotegui, "Morphological segmentation of building façade images," in *IEEE International Conference on Image Processing, ICIP'09*, 2009, pp. 4029–4032.
- [4] O. Teboul, L. Simon, P. Koutsourakis, and N. Paragios, "Segmentation of building facades using procedural shape priors," in *CVPR*, 2010, pp. 3105–3112.
- [5] K. Hammoudi, *Contributions to the 3D city modeling*, Ph.D. thesis, Université Paris-Est, 2011.
- [6] A. Pinte, C. Baillard, and E. Denis, "Modélisation de façades par analyse conjointe d'images terrestres et de données laser," *Revue française de photogrammétrie et de télédétection*, vol. 194, pp. 53–65, 2011.
- [7] G. Matheron, *Random Sets and Integral Geometry*, John Wiley & Sons, New York, 1975.
- [8] P. Maragos, "Pattern spectrum and multiscale shape representation," *IEEE Transactions on Pattern Analysis and Machine Intelligence*, vol. 11, pp. 701–716, 1989.
- [9] J. Serra, *Image Analysis and Mathematical Morphology*, vol. 2, Academic Press, London, 1988.
- [10] P. Soille, *Morphological Image Analysis: Principles and Applications*, Springer-Verlag New York, Inc., Secaucus, NJ, USA, 2003.